RESEARCH PAPER

PCCP
www.rsc.org/pccp

Electrical properties of short DNA oligomers characterized by conducting atomic force microscopy

Claude Nogues,[a] Sidney R. Cohen,[b] Shirley S. Daube[b] and Ron Naaman*[a]

[a] *Department of Chemical Physics, Weizmann Institute, Rehovot, 76100, Israel. E-mail: ron.naaman@weizmann.ac.il; Fax: 972-8-9344123; Tel: 972-8-9342367*
[b] *Chemical Research Support, Weizmann Institute, Rehovot, 76100, Israel*

Received 15th July 2004, Accepted 9th August 2004
First published as an Advance Article on the web 20th August 2004

Complementary, single-strands of DNA (ssDNA), one bound to a gold electrode and the other to a gold nanoparticle were hybridized on the surface to form a self-assembled, dsDNA bridge between the two gold contacts. The adsorption of a ssDNA monolayer at each gold interface eliminates non-specific interactions of the dsDNA with the surface, allowing bridge formation only upon hybridization. The technique used, in addition to providing a good electrical contact, offers topographical contrast between the gold nanoparticles and the non-hybridized surface and enables accurate location of the bridge for the electrical measurements. Reproducible AFM conductivity measurements have been performed and significant qualitative differences were detected between conductivity in single- and double-strand DNA. The ssDNA was found to be insulating over a 4 eV range between ±2 V under the studied conditions, while the dsDNA, bound to the gold nanoparticle, behaves like a wide band gap semiconductor and passes significant current outside of a 3 eV gap.

Introduction

While the primary biological function of DNA involves information storage and transfer, its unique structural properties can be exploited to build up molecular device structures. Amongst these characteristics are the specific and reversible interaction of complementary sequences of DNA oligomers, and the ease with which DNA can be synthesized and modified to comprise different lengths or contain functional groups that allow attachment to various surfaces.[1,2] However, an unsettled issue pertinent to the construction of molecular devices is precise determination of the electrical properties of DNA oligomers, and how these properties depend on various parameters such as the DNA length and sequence and whether the DNA is single or double stranded.

These issues were addressed in numerous studies by different groups.[3] Nevertheless, the results presented so far are largely inconsistent with each other, with DNA electrical behavior characterized as either insulating,[4–7] semi-conducting,[8] conducting,[9–12] or super-conducting.[13] The reasons for this disparity probably lie in the use of different DNA conformations, configurations and experimental conditions. In addition, many of the electrical measurements performed on long DNA oligomers, were done with the DNA lying flat on the surface. The interactions between the DNA and the surface (*via* either the π electrons of the bases, the phosphate groups or electrostatic forces) may affect both the DNA conformation and its electrical properties.[14] Recently, a review of this work has highlighted the length dependence on the electrical properties of DNA.[3] In all cases in which the DNA displayed charge transfer behavior, the DNA was less than 40 nm in length. When the DNA was longer than 40 nm it acted as an insulator. Another persistent problem in performing conduction experiments is the nature of the contacts between the molecule and the electrodes. In many of the studies the contact was only physical, namely the DNA was lying on the electrodes. Therefore some of the irreproducibility in the experiments could stem from the ill-defined electrical contacts.[15]

The experimental configuration described here was inspired by the work of Cui *et al.* who developed a method for measuring conductivity of single molecules.[16] They used thiol groups at both extremities of alkyl chains to make chemical bonds to a gold substrate on one end and a gold nanoparticle on the other. Electrical contact to the gold nanoparticle was made with a gold-coated atomic force microscopy tip. They demonstrated that having a chemical bond between the molecule and both electrodes is an essential condition to obtain reproducible and reliable *I–V* characterization. In the approach presented here, we have utilized the fact that thiolated ssDNA oligomers form self-assembled monolayers (SAMs) on a gold substrate under appropriate adsorption conditions.[17–19] ssDNA can similarly be attached to gold nanoparticles through the thiol bond.[20] When the ssDNA on the nanoparticles is complementary to that comprising the SAM on the flat gold substrate, the two strands can hybridize to form a nanoparticle –dsDNA–gold complex.[20] Therefore, the dsDNA oligomers are bound on one end to the gold surface (bottom electrode) while their outer ends are chemically bound to the gold nanoparticles (top electrode) in symmetrical fashion.

By making a self-assembled monolayer of ssDNA oligomers, we ensure that the dsDNA is not interacting with the substrate through the bases or phosphate groups.[18,19] In addition, the thickness of the layer can be easily measured. Location of the dsDNA is simplified due to the topographic contrast provided by the distinctive gold nanoparticle features, and accuracy is ensured as the gold colloids are only associated with the hybridized DNA.

Following extensive characterization, we applied conducting-atomic force microscopy (c-AFM) to qualitatively investigate the electrical properties of the sample. Results on the characterization of the DNA monolayers are presented as well as the conductivity measurements.

Experimental section

Gold substrate preparation

Gold evaporation onto silicon wafers: Polished n-type single crystal (111) silicon wafers (MOTOROLA, resistance: 10–15 Ω cm^{-2}) were cleaned by boiling in ethanol (Merck,

DOI: 10.1039/b410862k

Pro-Analysis) twice for 20 min and dried under Nitrogen. The wafers were immediately placed in an electron beam evaporator (EDWARDS, AUTO 306, TURBO) equipped with a thickness monitor (EDWARDS FTM7). The deposition was carried out at a base pressure of 5×10^{-6} mbar. A 1 nm chromium adhesive layer was deposited at a rate of 0.01 nm s^{-1}. The rate of the gold layer deposition (100 nm thick) was 0.01–0.03 nm s^{-1}.

Prior to the DNA adsorption the gold substrates were first rinsed twice in boiling ethanol for 20 min. After being dried under nitrogen they were immersed in hot piranha solution (3 : 1 H_2SO_4 : H_2O_2) for 10 min (*CAUTION: Piranha solution can react violently with organic material, and should be handled with extreme caution. Piranha solution should not be stored in tightly sealed containers*). They were then thoroughly rinsed with ultra pure water (Millipore, 18 MΩ). Only substrates that were perfectly wet by water were used in the DNA deposition.

Gold evaporation onto mica for AFM images and conductive AFM measurements: a 100 nm thick gold deposition was carried out at base pressure of 5×10^{-6} mbar on freshly cleaved Mica (Ruby mica, ASTM V-1 quality, S&J TRADING INC) at a rate of 0.01 nm s^{-1}. Prior to the molecular adsorption, the gold surface was cleaned by passing the sample through a flame with the gold facing up, followed by immersion in ultra-pure water. The substrate is tested as above for water wettability, and the flame treatment repeated if necessary. The gold substrate is then dried under nitrogen and placed into an empty test tube which is heated at 650 °C for 1 min in a flame. After the substrate has cooled down to ambient temperature, the DNA deposition is performed. This annealing procedure yields large, atomically smooth Au(111) terraces, as verified by STM and AFM images (not shown).

DNA adsorption

Reduction of thiolated ssDNA. 3′ thiolated DNA oligonucleotides were kept in their oxidized form-$(CH_2)_3$-S-S-$(CH_2)_3$-OH in order to protect the thiol group from undesired oxidation products or dimerization. Prior to adsorption, the amount of DNA needed for adsorption was incubated with 10 mM of the reducing agent Tris(2-carboxyethyl) phosphine (TCEP) in 100 mM Tris-HCl, pH 7.5. The mixture was incubated at room temperature for several hours to allow complete reduction of the disulfide bond. The DNA samples were then passed through a column (BioSpin 6, BioRad) pre-equilibrated with the buffer used for the DNA adsorption (0.4 M NaH_2PO_4, pH 7.4). The high molecular weight DNA molecules were collected in the flow through in adsorption buffer, while small molecular weight species (TCEP and the reduction product HS-(CH_2)-OH, the latter may compete with the DNA for binding to the gold) were captured on the spin columns. The final ssDNA concentration was adjusted to 10 μM. The flow-through samples were pipetted immediately onto the clean gold slides. The DNA sequence used to form monolayer on the flat gold surface was: 5′-CAT-TAA-TGC-TAT-GCA-GAA-AAT-CTT-AG-3′. The following complementary sequence was used to form a monolayer on gold nanoparticles: 5′-CTA-AGA-TTT-TCT-GCA-TAG-CAT-TAA-TG-3′.

ssDNA oligonucleotide adsorption on flat gold surfaces. 10 to 15 μl of the 10 μM reduced DNA solution was pipetted onto the clean gold surface (either gold on silicon or gold on mica). The gold samples were then placed in a sealed Petri dish at 100% relative humidity to avoid drying of the DNA solution. After 2 h of adsorption the samples were rinsed by 20 min incubation in the adsorption buffer. This rinsing procedure was performed three times in order to remove excess DNA. The samples were then thoroughly rinsed with sterile ultra-pure water in order to remove excess salt remaining on the surface. Samples were kept in sterile ultra-pure water and were dried under nitrogen just prior to characterization.

ssDNA adsorption on gold nanoparticles (GNP). The GNP (Aldrich – nominal 10 ± 3 nm diameter) were rinsed with deionized water by two centrifugations at 8000 rcf. After the water surfactant was removed, 200 μl of 10 μM of reduced thiolated ssDNA diluted in sterile deionized water was added to the GNP. The mixture was stirred overnight at room temperature. Following incubation, the GNP were rinsed with water and Tris (0.025 M)–NaCl (0.2 M pH 7.5) buffer by one centrifugation cycle at 10 000 rcf. The GNP labeled ssDNA (GNP-ssDNA) in 0.2 M buffer was agitated for 4 hours at room temperature, followed by rinsing twice in Tris (0.025 M)–NaCl (0.4 M). GNP–ssDNA solutions were kept in the same buffer at 4 °C.

DNA hybridization on the surface

10 to 15 μl of the GNP–ssDNA diluted in a Tris (0.025 M)–NaCl (0.4 M) buffer were dropped onto the ssDNA monolayer on gold. The sample was then placed in a sealed Petri dish at 100%-relative humidity as above. After 12 h of incubation each sample was rinsed three times for 20 min, with the Tris (0.025 M)–NaCl (0.4 M pH 7.5) buffer to remove excess of GNP–ssDNA. Prior to characterization, each sample was rinsed with sterile deionized water to remove excess salt.

Radioactivity measurements

In order to characterize the density of the ssDNA on the surface, radioactive phosphate was used to label the DNA at its 5′ end, following a published procedure.[21] After 2 h of incubation the monolayers were rinsed by incubating 3 times for 20 min in the adsorption buffer and 3 times for 20 min in sterile water. The specific activity of each DNA sample is defined as the amount of radiation produced by a mole of that DNA. This number was determined by dropping 1 μl samples of radioactive DNA on a gold reference slide. These calibration samples were allowed to air dry without any washing, followed by phosphor-imaging (BAS-2500, Fuji). The amount of pixels at each spot was divided by the amount of pMoles pipetted, yielding the specific activity of the samples.

AFM measurements

The monolayer was imaged in air under ambient conditions (22 °C and 60% relative humidity) using a Digital Instruments NS IIIa Multimode AFM operating in Tapping Mode™. The silicon probes (Olympus OTESP) used possessed a resonance frequency of 280–380 kHz and a nominal force constant of 30 N m^{-1}. For c-AFM measurements an NT-MDT P47 Solver was used. The conducting, Pt-coated silicon probes (Mikro-Mash CSC12/Ti-Pt), had a range of force constants. The stiffer of these cantilevers, possessing nominal spring constants of 0.4–2 N m^{-1} and resonance frequency of 60–200 kHz could be used in both contact and intermittent-contact modes (here, intermittent-contact and Tapping Mode™ are used interchangeably).

In order to measure current flow between tip and sample, an electrically conductive probe at the input of a current-voltage amplifier is scanned over the DC-biased sample surface. Typically, this measurement is made in contact mode while the feedback loop keeps the deflection of the cantilever and hence tip-sample force constant. Measuring current when the operating mode is intermittent-contact is problematic: The current amplifier is relatively slow and can only detect currents in the time regime from DC up to several kHz. It is therefore not useful for measuring an intermittent current which may exist during the brief contact part of the cycle in intermittent-contact

mode, for the probes used here with typical resonance frequencies over 100 kHz. As described in more detail below, under sufficiently low setpoint (larger average force), a pseudo-DC current can be measured to give current mappings together with the intermittent-contact image.

In addition to current mappings, c-AFM allows measurement of local current–voltage (I–V) curves using the spectroscopy mode. These are performed at a single surface spot by ramping the tip-surface bias while recording the current and without any sideways motion of the tip which could cause damage on the surface through shear.

Results and discussion

System characterization

In order to approach the idealized junction configuration depicted in Fig. 1 several requirements have to be fulfilled: The original ssDNA coverage on the surface should be dense enough to prevent nonspecific interactions of the dsDNA backbone with the metal after hybridization;[18,19,22] however it should be loose enough to allow efficient hybridization with the complementary strand bound to the GNP.[23] A well-defined oligomer conformation at the surface requires binding through the thiol linkage. The adsorbed ssDNA oligomers on the gold substrates were characterized by AFM in tapping mode as well as by radiolabeling.

The kinetics of thiolated ssDNA adsorption on gold was reported in previous works.[19,24,25] It was shown that the DNA oligomers adsorb in a two-step process, the first 30 min of adsorption are characterized by rapid adsorption, followed by an adsorption, desorption and diffusion (ADD) stage.[19] For long adsorption times the ssDNA coverage corresponds to the high coverage not suitable for the purpose of hybridization, as the hybridization yield is highly dependent on the density of the immobilized ssDNA.[23] Our radio-labeling experiments performed with ssDNA 26 bases long indicated that a density

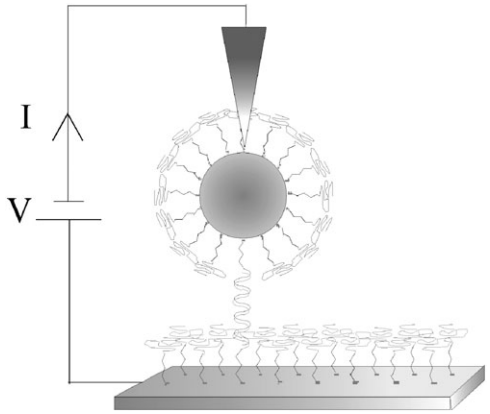

Fig. 1 Schematic of a single-strand DNA (ssDNA) monolayer on gold electrode and the double-strand DNA (dsDNA) bridge between the gold substrate and the gold nanoparticle formed through hybridization.

of $3 \pm 0.4 \times 10^{13}$ molecules cm^{-2} had been reached after 2 h of adsorption, compared to $1.2 \pm 0.5 \times 10^{12}$ molecules cm^{-2} for the non-thiolated ssDNA. Hence, the non-specific binding (nucleotide–gold interaction with no chemisorption *via* the thiol group) corresponds to less than 4% of the adsorbed DNA. Fig. 2 shows a 1 μm^2 AFM image of a gold surface exposed for 2 h to a 10 μM ssDNA solution in phosphate buffer 0.4 M, pH 7.4. The surface is homogenous (Fig. 2a) and displays close-packed protrusions with an apparent diameter of 20 nm (Fig. 2b). The apparent diameter of the structure reflects the size and shape of the tip. The peak to peak vertical roughness indicated in the cross-section is *ca.* 1 nm. This structure is consistent with an adsorbed monolayer film of the oligonucleotides.[26,27]

Fig. 3 shows a 1 μm-wide image of the previous sample after incubation of the ssDNA monolayer with the GNP labeled

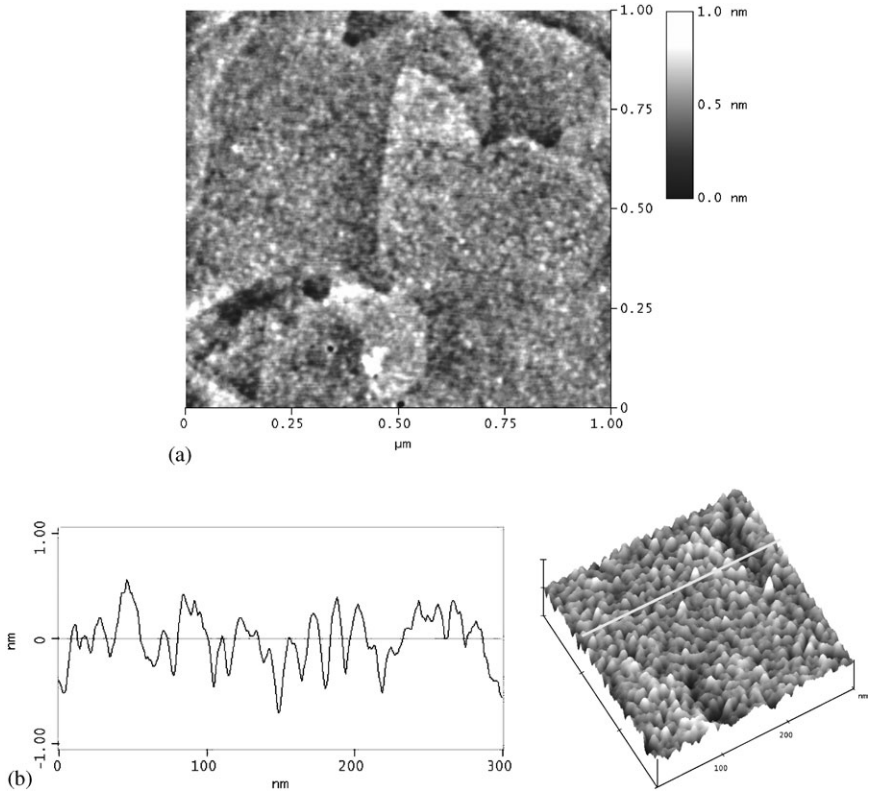

Fig. 2 (a) Tapping mode AFM (TM-AFM) scan of a pure ssDNA monolayer adsorbed on Au(111) on mica surface, xy scale 1 μm and z scale 8 nm. The adsorption time for the monolayer formation is 2 h. (b) Cross section of a 300 nm line segment revealing typical vertical roughness of 1 nm.

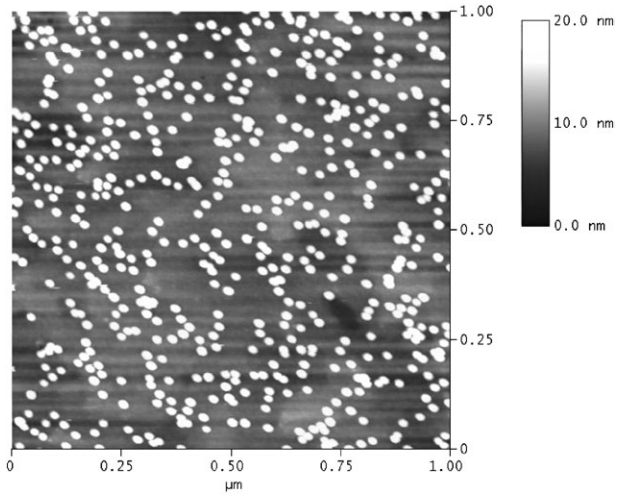

Fig. 3 TM-AFM image of a ssDNA-modified gold substrate after incubation with gold nanoparticle-labeled with the complementary strand (Au-dsDNA-GNP). Average gold nanoparticle number density = 450 μm^{-2}.

with the complementary ssDNA. This image was taken after rinsing the surface with Tris–NaCl buffer for 1 hour, which is sufficient to remove GNPs which are not bound by hybridization. Initially, a brief rinse with water was performed to remove the excess salt left on the surface from the buffer. Thus, the number of gold particles detected on the surface reflects the hybridization yield.[23] In most of the cases the GNP density on the surface was too high for the c-AFM measurements, where isolated GNPs are needed. Further rinsing with water washes off more GNPs by denaturing the double stranded DNA. After 5 min of rinsing, the GNP density corresponds to an average of 450 gold nanoparticles per 1 μm^2 suitable for our measurements (Fig. 3). No agglomeration of the gold nanoparticles is observed indicating that the non-specific interaction between the ssDNA modified nanoparticles on the surface is minimized. Control experiments, whereby the gold nanoparticles were modified with non-complementary ssDNA strands, displayed very few gold nanoparticles on the surface, on the order of 5 gold nanoparticles per μm^2 (see below). Here, the water rinse was very brief to avoid washing away all the GNPs.

The mechanical stability of the bound GNPs provides a further concern: a series of experiments (not shown) showed that scanning in contact mode did not remove the ssDNA monolayer adsorbed on the flat gold but completely swept away the gold nanoparticles. The lateral force applied during the contact mode scan was estimated to be several tens of nN. This value is higher by over an order of magnitude from the previously estimated 150 pN required for breaking the hybridization in an isolated dsDNA molecule.[28–31] These results demonstrate why the conventional conductive AFM technique performed with a constant contact force is not appropriate for the measurements proposed here.

Conductivity measurements

To overcome the inability to use traditional contact mode c-AFM measurements, intermittent-contact mode was used. In order to perform conduction measurements within the time response limitations of the current measurement, the setpoint in the intermittent-contact mode was significantly reduced so that during most of the oscillation cycle the tip was in contact with the surface. The physical meaning of such experimental conditions is that shear forces are eliminated since the tip lifts briefly from the surface during each oscillation cycle, yet the tip is in intimate contact with surface most of the time, so that an averaged, DC current is measured. Although these

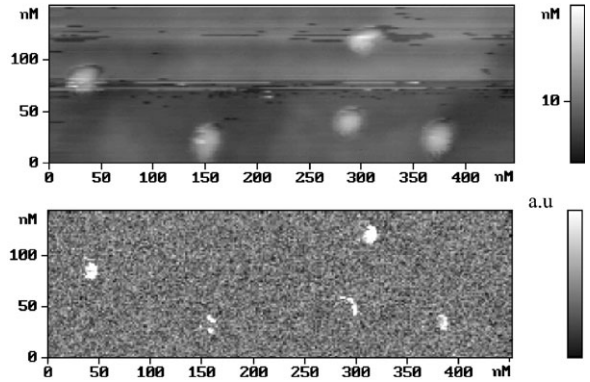

Fig. 4 Intermittent-contact c-AFM image of the Au-dsDNA-GNP sample using a conducting tip at a low setpoint; (a) height, (b) current response at +2.8 V sample bias.

measurements allow a qualitative mapping of the conductivity, the current magnitude is a complicated convolution of the amplifier response time, frequency of oscillation, and unknown time period of the contact. Therefore, the current magnitudes shown in Figs. 4–6 cannot be compared with current magnitudes observed for *I–V* curves under constant contact force (*vide infra*). Topography and current images of the ssDNA monolayer incubated with the gold nanoparticles labeled with the complementary strand are shown in Figs. 4a and 4b, respectively. In the topography image one can easily distinguish 5 isolated gold nanoparticles bound to the flat gold surface *via* the dsDNA. Here, the quality of the topography images is degraded relative to Figs. 2 and 3 due to the extra tip

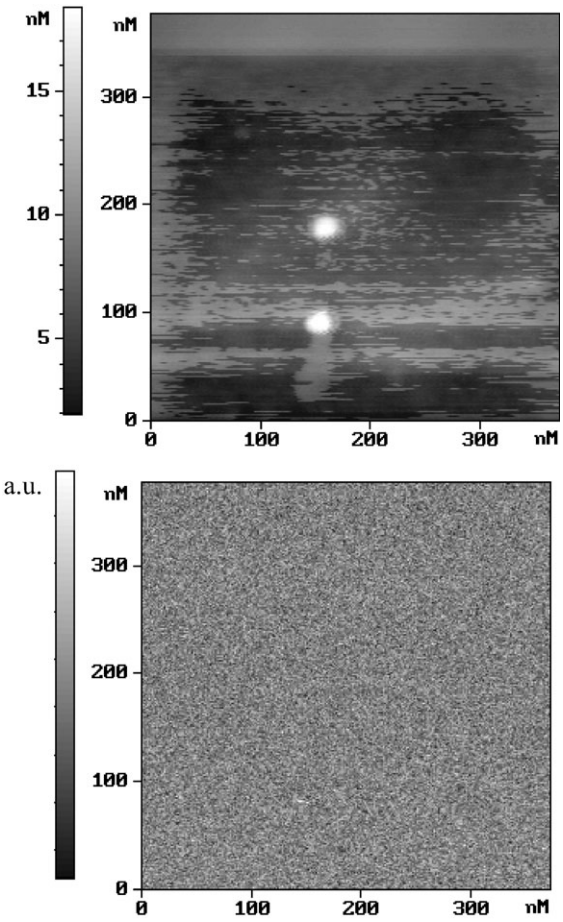

Fig. 5 Intermittent-contact c-AFM image of a DNA-modified gold substrate after incubation with gold nanoparticle-labeled non-complementary DNA; (a) height, average gold nanoparticle density = 2–3 per 500 × 500 nm^2, (b) current response at a +2.8 V sample bias.

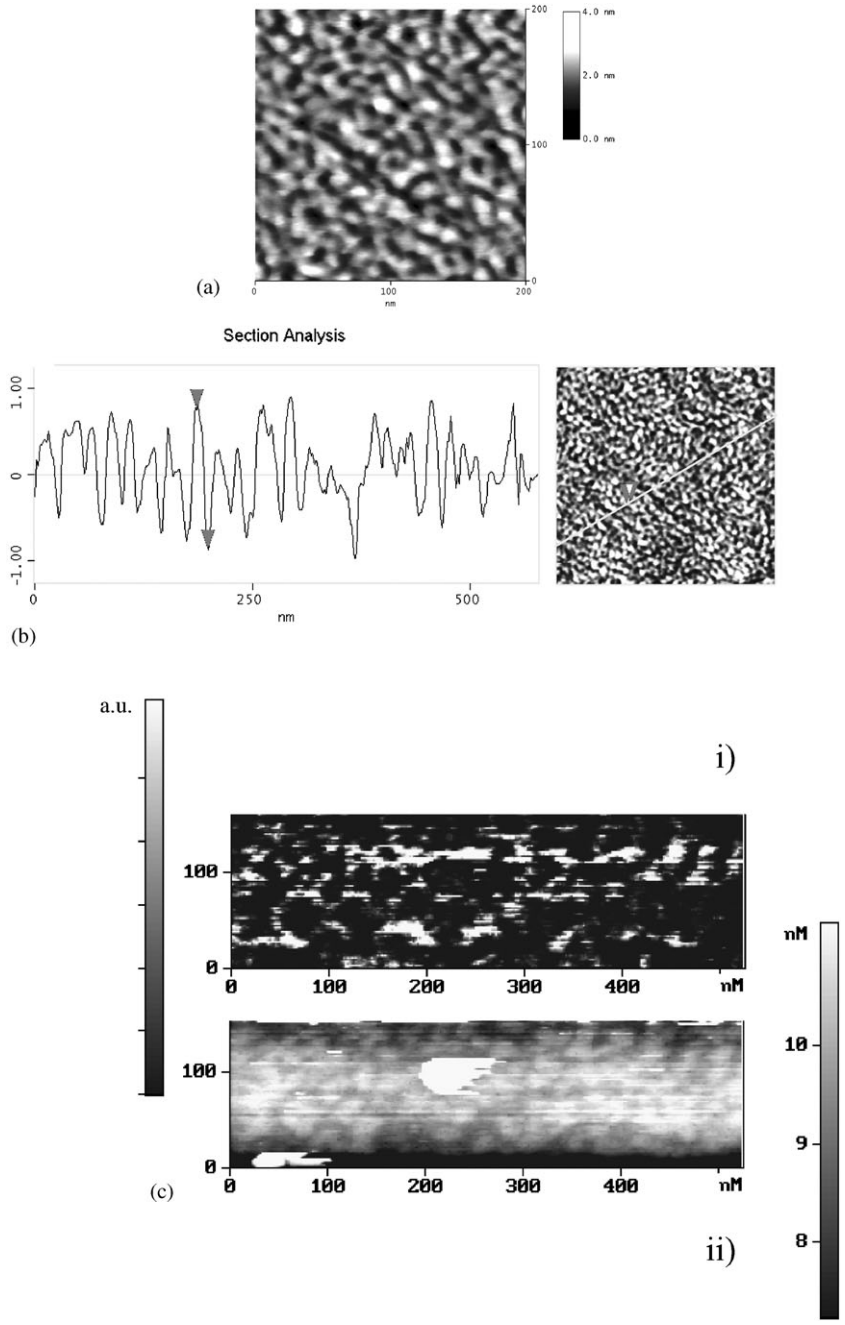

Fig. 6 (a) TM-AFM image of a mixed ssDNA/6-mercaptohexanol monolayer on Au(111). The adsorption solution was composed of 50% of each component at 10 μM concentration, scan size = 200 nm; (b) cross section of a 500 nm scan revealing domains with a difference in height of 2 nm; (c) intermittent contact-c-AFM image of the mixed monolayer after incubation with 10 nm gold nanoparticle-labeled non-complementary ssDNA; i - current response at +2.8 V sample bias, ii - height.

bulk caused by the metal coating. The corresponding current image (Fig. 4b) shows that current flows only at locations of the gold nanoparticles. In-between the gold nanoparticles no current signal was recorded. As a control, the same experiment was performed on a sample where the gold particles are coated with non-complementary ssDNA (Fig. 5a). It can be seen that there are less gold nanoparticles on the surface, compared to the previous sample where the two DNA strands were complementary (compare Fig. 5a to Fig. 3). In the corresponding current image (Fig. 5b) no current was detected above the noise level.

From the measurements displayed in Figs. 4 and 5, we conclude that current is measured only when the GNPs are labeled with a strand complementary to the one adsorbed on the flat gold surface.

We now address the question of whether the DNA remains double stranded under the conditions used for the AFM measurements. A stable dsDNA requires bound counter-ions and water molecules as part of the helical structure. It has been shown recently that these structural parameters hold even after drying under desiccant.[32] Since the present studies were performed at ambient temperature with humidity reaching 60%, it is safe to assume that enough water molecules and counter ions are left to keep a helical structure. Furthermore, reports concerning DNA characterization by STM under vacuum show that one can clearly distinguish between single and double stranded DNA.[33] Finally, and most importantly, had the DNA been denatured upon drying of the sample, there would not have been such a difference in the current images of complementary and non complementary GNPs.

We now consider the possibility that the current is ionic. In the case of non-complementary oligomers (Fig. 5), in order not to remove all the gold nanoparticles, the water rinsing was kept to a minimum. Under these conditions, the amount of salt left

from the buffer is higher than for the sample with the complementary strands, where the rinsing was extensive. Because we do not detect any current signal from the ssDNA monolayer at 60% humidity (with a few experiments at 40% humidity showing similar behavior), it is therefore safe to conclude that there is no ionic current. We can also rule out direct tunneling between upper (tip) and lower (substrate) electrodes as providing the difference between ss and dsDNA: Considering the exponential dependence of tunneling current on distance for a planar tunnel junction,[34] larger current would imply a smaller barrier width for the dsDNA. In fact, the measured distances are similar in the two cases, and the thickness of the ssDNA monolayer, measured by ellipsometry, was found to be 33 ± 5 Å, which presents an exceptionally wide tunneling barrier. As a consequence, the current must be transferred through the dsDNA strand.

To demonstrate that the absence of current is an intrinsic property of the ssDNA and not due to changes in tip conductivity, an additional control experiment was performed. Measurements were made on a mixed monolayer formed by a 2 h immersion in a solution of 50% ssDNA and 50% 6-mercaptohexanol at a total concentration of 10 μM. This film exhibits clear domain separation into the two components as seen in the height image and zoomed-in cross-section of Figs. 6a and 6b, with domains of the DNA oligomers rising about 2 nm higher than those of the 6-mercaptohexanol. Fig. 6c presents topography and current images measured simultaneously with a conductive tip on this sample. The two gold nanoparticles present on this surface are covered with the **non**-complementary strands. Current is present in the domains of the short thiols, but not on the ssDNA domains, as seen by the correspondence of current flow (bright regions) with lower topography. The current flow is by tunneling, as the height of a 6-mercaptohexanol oriented normal to the surface is only 8 Å. No current can be detected where the gold nanoparticles are located on the surface. This control experiment further confirms that in order to detect any current flow, double stranded DNA is required.

Although the above experiments show that the presence of dsDNA is essential for current flow, they do not provide any quantitative indication of the current or resistance of the system. In order to obtain spectroscopic information on a particular surface site, without brushing the gold particle away, experiments were performed where a nanoparticle was first centered in a small scan zone. The system was then transformed smoothly from intermittent into contact mode without any lateral motion which would disrupt the surface by shear. Directly after making this soft contact, *I–V* spectroscopic measurements were made. In Fig. 7 consecutive *I–V* curves are shown, measured on one GNP bound to the gold substrate through the hybridization process. The two consecutive *I–V* curves measured show significant current flow above a bias of ±1.5 V (Figs. 7a and 7b). At 2 V the current reaches 4 nA and the resistance measured from the slope of the curve at 1.8 V is *ca.* 0.4 GΩ. Between ±1 V the resistance is nearly two orders of magnitude larger (*ca.* 10 GΩ). This behavior was reproducible for up to 6 consecutive *I–V* measurements on a single GNP.

Considering the constraints placed on the number of DNA molecules that can hybridize between the surface and the GNP due to molecular length, monolayer height, and the size and shape of the GNP, we can estimate an upper limit for the number of molecules that form the bridge. Geometrically, it is reasonable to estimate that only the bottom 1/3 of the total area of the GNP is available for hybridization. This corresponds to an area of 105 nm^2, therefore for 100% hybridization, 30 such DNA bridges could exist (3.33 nm^2 molecular cross-section). In reality, the percent hybridizing will be much lower: Peterson *et al.* found a maximum of less than 50% for 3×10^{12} probes cm^{-2}.[35] Here, the packing density is more than ten times this value, and radioactivity measurements indicate hybridization efficiencies of *ca.* 10% due to more stringent space restrictions. Since the GNP introduces further steric constraints, a maximum of 10% hybridization efficiency could be considered. Thus the average number of dsDNA under each GNP is *ca.* 3. Consequently, the current that flows through individual dsDNA is between 0.2 and 1.4 nA per dsDNA at voltage bias of 1.5–2 V. This result agrees well with previous, preliminary values obtained for short oligomers in the experiments of Porath *et al.*,[8] Watanabe *et al.*[10] and Shigematsu *et al.*[11] obtained under less stringent control of current path and quality of molecular contact.

Identical *I–V* curves were also obtained when the measurements were done on different gold nanoparticles on the same sample and on different samples. The small current hysteresis around 0 V is due to a capacitive coupling in the measuring system, which is seen on all samples measured and varies with the rate of the bias sweep.

The first *I–V* curve measured on a GNP often shows insulating behavior between −2 and +2 V. This could be due to slight contamination residues on the tip, which are removed upon application of a voltage sweep,[36] or penetration of the tip into the ssDNA layer present on the GNP in order to make a good electrical contact. Whereas this initial conditioning response is assigned to improvement of the electrical contact between the AFM tip and the GNP, the next 4–6 consecutive measurements remain invariant, as represented in Figs. 7a and 7b, showing that no irreversible damage of the dsDNA bridge

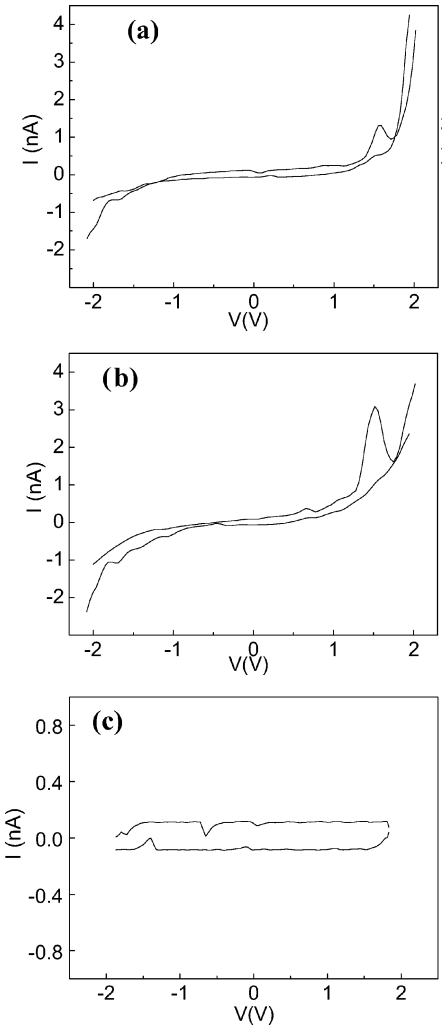

Fig. 7 (a, b) Consecutive *I–V* curves characteristic of the Au-dsDNA-GNP bridge measured by c-AFM (see text). (c) *I–V* curve measured directly on the ssDNA monolayer. Note the expanded current scale relative to a, b.

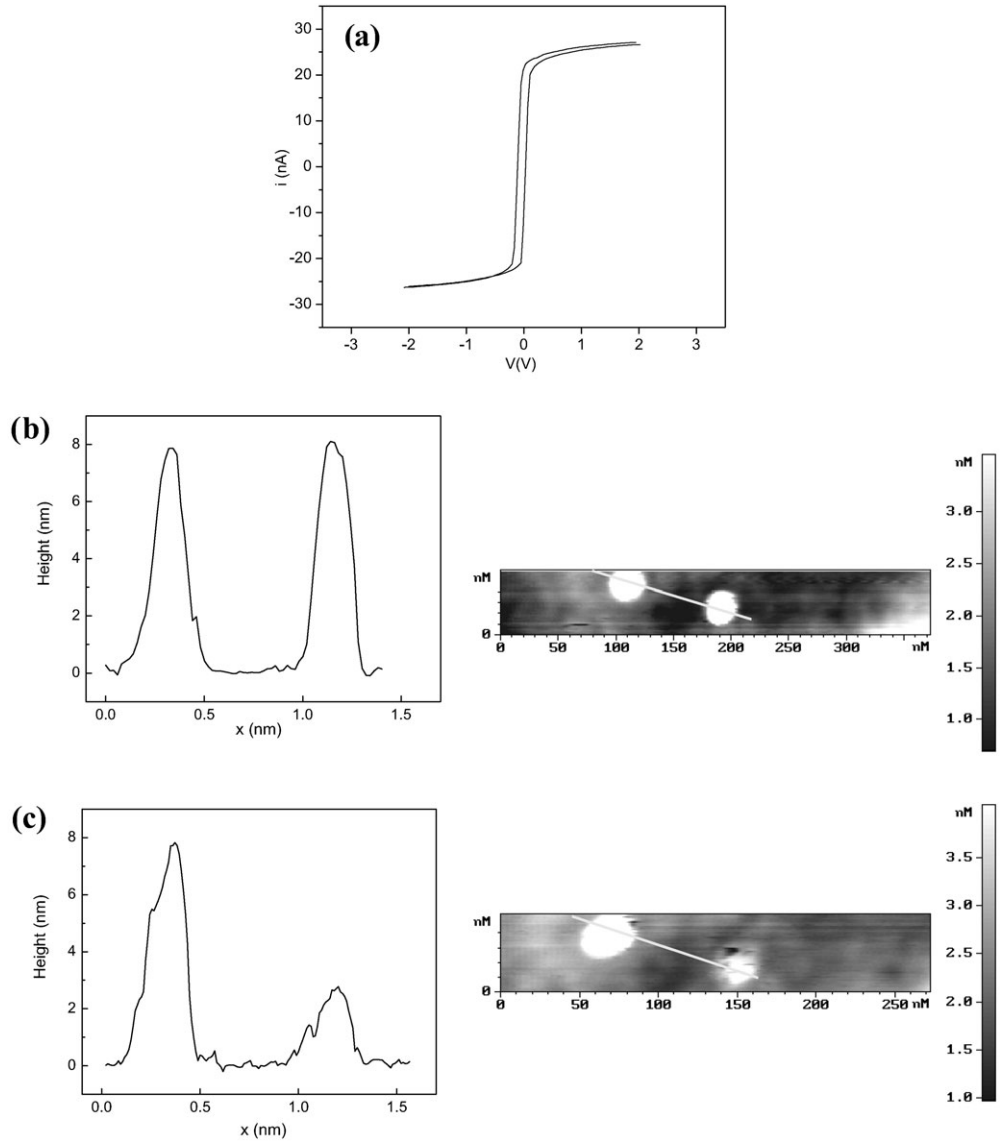

Fig. 8 (a) *I–V* curve obtained on the Au-dsDNA-GNP after 6 consecutive *I–V* scans (as measured in Fig. 7a,b). The current amplifier saturates above 20 nA. Topography image and horizontal cross section of the GNP before (b) and after (c), the series of *I–V* curve measurements.

occurred at this stage. After this, the *I–V* curve of Fig. 8a is obtained, indicating a direct electrical contact between the tip and the gold substrate, with resistance of *ca.* 3 MΩ around 0 V bias. This transition can be understood from the images of Figs. 8b,c. Here, the topography and cross-section of the GNP directly before (b) and just after (c) the 6 consecutive , *I–V* curves were measured. The apparent height of the probed GNP decreased from 10 to 4 nm. The current transition can thus be ascribed to the force applied by the tip on the gold nanoparticle, which pushes the nanoparticle till it touches the flat gold surface. This topographical change could be an indicator for damage to the dsDNA bridge. We are confident that this damage occurs only *after* the *I–V* curves of Fig. 7a,b because of the preliminary, repeatable experiments shown both in Figs. 4 and 5, and on the mixed monolayer described on the bottom of page 13. In addition, we note the repeatability of the *I–V* curves on the dsDNA, until the catastrophic failure seen in Fig. 8a. When comparable measurements are taken directly on the ssDNA monolayer, no current is detected within the range of ±2 V (Fig. 7c) confirming the fact that the ssDNA monolayer, is an insulator under the present experimental conditions. This behavior was invariant for repeated *I–V* curves on the same spot.

The results confirm that the detected current flows only through the dsDNA. An exciting observation is that the sharp peaks in the conducting region are reproducibly obtained and may point to distinct electronic states. This point is currently under closer study.

Conclusion

This paper describes how the interaction between two complementary DNA strands can be exploited in order to self-assemble a DNA bridge between a flat gold surface and a gold nanoparticle. A ssDNA is adsorbed onto the flat gold surface while the complementary strand is chemisorbed onto the gold nanoparticle. The final structure is formed through the hybridization of the two single strands into a double strand. The specific binding of functionalized dsDNA to both gold electrodes is made *via* the chemical thiol–gold linkage.

After hybridization, the dsDNA molecules stretch away from the surface within a monolayer of insulating ssDNA. Therefore any non-specific interaction between the dsDNA and the gold surface is sterically prevented by the ssDNA monolayer. This has enabled accurate, repeatable measurements of the conductivity of isolated double stranded DNA molecules, revealing meaningful differences between the conductivity of single- and double-strand DNA. The ssDNA was found, under the present experimental set-up, to be insulating over a 4 eV range of ±2 V, while the dsDNA passes significant current

outside of a 3 eV gap. These results are in qualitative agreement with the predicted gap in DNA.[37]

The novel approach described here provides the opportunity to investigate the influence of different parameters on DNA charge transfer properties under experimentally repeatable conditions. For example, as has been shown in previous reports, the DNA length can dramatically modify the electrical properties of the DNA by increasing the probability of defects within the chain. Furthermore, one of the more exciting issues, still requiring experimental quantification, is the influence that the DNA base sequence has on its charge transfer properties.

Acknowledgements

We acknowledge helpful discussions with Dr Danny Porath and Hezy Cohen. CN acknowledges the support as a Marie-Curie fellow. CN and RN acknowledge partial support from the EU under the SENTIMATS project and from the Israel Ministry of Science.

References

1 B. Kasemo, *Surf. Sci.*, 2002, **500**, 656.
2 M. J. Tarlov and A. B. Steel, in *Biomolecular Films: Design, Function, and Applications*, ed. J. F. Rusling, Marcel Dekker, New York, 2003, vol. 111.
3 D. Porath, G. Cuniberti and R. Di Felice, *Top. Curr. Chem.*, 2004, **237**, 183.
4 E. Braun, Y. Eichen, U. Sivan and G. Ben-Yoseph, *Nature (London)*, 1998, **391**, 775.
5 Y. Zhang, R. H. Austin, J. Kraeft, E. C. Cox and N. P. Ong, *Phys. Rev. Lett.*, 2002, **89**, 198102.
6 P. J. de Pablo, F. Moreno-Herrero, J. Colchero, J. Gómez Herrero, P. Herrero, A. M. Baró, P. Ordejón, J. M. Soler and E. Artacho, *Phys. Rev. Lett.*, 2000, **85**, 4992.
7 A. J. Storm, J. van Noort, S. de Vries and C. Dekker, *Appl. Phys. Lett.*, 2001, **79**, 3881.
8 D. Porath, A. Bezryadin, S. De Vries and C. Dekker, *Nature (London)*, 2000, **403**, 635.
9 H. W. Fink and C. Schönenberger, *Nature (London)*, 1999, **398**, 407.
10 H. Watanabe, C. Manabe, T. Shigematsu, K. Shimotani and M. Shimizu, *Appl. Phys. Lett.*, 2001, **79**, 2462.
11 T. Shigematsu, K. Shimotani, C. Manabe, H. Watanabe and M. Shimizu, *J. Chem. Phys.*, 2003, **118**, 4245.
12 B. Xu, P. Zhang, X. Li and N. Tao, *Nano. Lett.*, 2004, **4**(6), 1105.
13 A. Y. Kasumov, M. Kociak, S. Guéron, B. Reulet, V. T. Volkov, D. V. Klinov and H. Bouchiat, *Science (Washington, D. C.)*, 2001, **291**, 280.
14 A. Y. Kasumov, D. V. Klinov, P. E. Roche, S. Gueron and H. Bouchiat, *Appl. Phys. Lett.*, 2004, **84**(6), 1007.
15 K. W. Hipps, *Science (Washington, D. C.)*, 2001, **294**, 536.
16 X. D. Cui, A. Primak, X. Zarate, J. Tomfohr, O. F. Sankey, A. L. Moore, A. T. Moore, D. Gust, G. Harris and S. M. Lindsay, *Science (Washington, D. C.)*, 2001, **294**, 571.
17 E. Huang, M. Satjapipat, S. Han and F. Zhou, *Langmuir*, 2001, **17**, 1215.
18 T. M. Herne and M. J. Tarlov, *J. Am. Chem. Soc.*, 1997, **119** 8916.
19 R. Georgiadis, K. P. Peterlinz and A. W. Peterson, *J. Am. Chem. Soc.*, 2000, **122**, 3166.
20 A. Csaki, R. Moller, W. Straube, J. M. Kohler and W. Fritzsche, *Nucleic Acids Res.*, 2001, **29**, e81.
21 T. Aqua, R. Naaman and S. Daube, *Langmuir*, 2003, **19**, 10573.
22 A. B. Steel, R. L. Levicky, T. M. Herne and M. J. Tarlov, *Biophys. J.*, 2000, **79**, 975.
23 J. H. Watterson, P. A. E. Piunno, C. C. Wust and U. J. Krull, *Langmuir*, 2000, **16**, 4984.
24 E. M. Southern, S. C. Case-Green, J. K. Elder, M. Johnson, K. U. Mir, L. Wang and J. C. Williams, *Nucleic Acids Res.*, 1994, **22**, 1368.
25 C. Bamdad, *Biophys. J.*, 1997, **75**, 1997.
26 D. Erts, B. Polyakov, H. Olin and E. Tuite, *J. Phys. Chem. B*, 2003, **107**, 3591.
27 N. Mourougou-Candoni, C. Naud and F. Thibaudau, *Langmuir*, 2003, **19**, 682.
28 C. Bustamante, S. B. Smith, J. Liphardt and D. Smith, *Curr. Opin. Struct. Biol.*, 2000, **10**, 279.
29 M. C. Wiliams and L. Rousina, *Curr. Opin. Struct. Biol.*, 2002, **12**, 336.
30 R. Krautbouer, M. Rief and E. G. Hermann, *Nano Lett.*, 2003, **3**, 493.
31 T. Strunz, K. Oroszlan, R. Schäfer and H. J. Güntherodt, *Proc. Natl. Acad. Sci. U. S. A.*, 1999, **96**, 11277.
32 S. G. Swarts, M. D. Sevlla, D. Becker, C. J. Tokar and K. T. Wheeler, *Radiat. Res.*, 1992, **129**, 333.
33 S. Tanaka, S. Fujiwara, H. Tanaka, M. Taniguchi, H. Tabata, K. Fukui and T. Kawai, *Chem. Commun.*, 2002, **20**, 2330.
34 R. Wiesendanger, *Scanning Probe Microscopy and Spectroscopy Methods and Applications*, University Press, Cambridge, 1994, ch. 1.
35 A. W. Peterson, L. K. Wolf and R. M. Georgiadis, *J. Am. Chem. Soc.*, 2002, **124**, 14601.
36 S. R. Cohen, G. Neubauer and G. M. McClelland, *J. Vac. Sci. Technol., A*, 1990, **8**, 3449.
37 M. Hjort and S. Stafström, *Phys. Rev. Lett.*, 2001, **87**, 228101.

